Journal of Power Sources 232 (2013) 310–322

Contents lists available at SciVerse ScienceDirect

Journal of Power Sources

journal homepage: www.elsevier.com/locate/jpowsour

Review

A review of hollow Pt-based nanocatalysts applied in proton exchange membrane fuel cells

Xinwen Zhou*, Yali Gan, Juanjuan Du, Danni Tian, Ronghua Zhang, Changying Yang, Zhongxu Dai*

College of Chemistry and Life Science, China Three Gorges University, Yichang 443002, China

HIGHLIGHTS

- We present a review of the progress made for synthesizing hollow Pt-based nanocatalysts applied in PEMFCs.
- Hollow pure Pt catalysts, Pt-based alloy catalysts and other correlative hollow precious nanomaterials are reviewed.
- The methods used to synthesize hollow Pt-based nanocatalysts are summarized and compared.
- Galvanic replacement method is the most used and prospective method in this field.
- The emergent challenges and future developments of hollow Pt-based nanocatalysts are discussed.

ARTICLE INFO

Article history:
Received 24 October 2012
Received in revised form
14 December 2012
Accepted 14 January 2013
Available online 5 February 2013

Keywords:
Proton exchange membrane fuel cells
Hollow
Platinum based nanocatalysts
Galvanic replacement reaction

ABSTRACT

Proton exchange membrane fuel cells (PEMFCs) have found a wide variety of commercial applications to resolve the energy crisis and environmental pollution. Then the design of novel Pt-based catalysts with enhancing catalytic activity, stability and low amount of Pt used are crucial. Pt-alloy catalysts, core-shell structured Pt-based catalysts, Pt-monolayer catalysts, Pt-based catalysts with high index, nanoporous Pt-based catalysts, hollow Pt-based nanocatalysts, and non-noble catalysts are the common way to resolve the question partly. Among these catalysts, hollow Pt-based catalysts used in PEMFCs have received much attention due to the increased surface area, low density, improved utilization of the unit Pt. In this review, we present a summarization of the progress made for synthesizing hollow Pt-based nanocatalysts using different techniques. Hollow pure Pt catalysts, Pt-based alloy catalysts and other correlative hollow precious nanomaterials are covered. Galvanic replacement method is still the most used and prospective method in this field. Finding facile and appropriate sacrificial template and controllable shape will be the key in the development of this method. We also summarize other different methods and discuss the foreground of these methods in the future. The emergent challenges and future developments of hollow Pt-based nanocatalysts are also discussed in this paper.

1. Introduction

Fuel cell produces electricity from the electrochemical oxidation of hydrogen or small organic molecules, such as ethanol, formic acid, and methanol or other fuels. The cathode oxygen reduction reaction (ORR) and anode feed oxidation reaction both occur on the surfaces of catalysts. The commercialization of fuel cells is regarded as the most promising way to resolve the problems of increasing energy requirements, continuous and rapid depletion of conventional fossil fuels, environmental pollution, which were derived from the highly development of our society [1,2]. There are six main types of fuel cells, including (1) proton exchange membrane fuel cell (PEMFC) including direct methanol fuel cell (DMFC), (2) alkaline fuel cell (AFC), (3) phosphoric acid fuel cell (PAFC), (4) molten carbonate fuel cell (MCFC), (5) solid oxide fuel cell (SOFC) and (6) microbial fuel cell (MFC) [3]. The biggest advantage of PEMFCs over internal combustion engines in automotive vehicles is the fact that PEMFCs produce zero emissions when using hydrogen as the fuel and air as the oxidant. Recently, Debe et al. [4] concluded that PEMFCs have brought the technology close to pre-commercial viability, based on the current performances of the small test fleets of vehicles powered by automotive fuel cells. Pt-based catalysts are currently the only choice of electrocatalysts in practical PEMFCs until now. The high cost of PEMFCs especially the anode catalysts is one of the major challenges hindrance its

* Corresponding authors. Tel.: +86 717 6395580; fax: +86 717 6395516.
E-mail addresses: xwzhou@ctgu.edu.cn (X. Zhou), Daizx@ctgu.edu.cn (Z. Dai).

0378-7753/$ – see front matter © 2013 Elsevier B.V. All rights reserved.
http://dx.doi.org/10.1016/j.jpowsour.2013.01.062

commercialization. Then the design of novel Pt-based catalysts with enhancing catalytic activity, stability and low amount of Pt used are crucial in the commercialization of PEMFCs.

In recent years, hollow nanostructured materials used as electrocatalysts in PEMFCs have received much attention due to the increased surface area, low density, improved utilization of the unit Pt, which make them exhibit catalytic activities different from their solid counterparts [5,6]. In this review, we will focus on the design and fabrication of hollow Pt-based nanocatalysts and their applications in PEMFCs. Also, we discuss the general methods for fabrication of hollow Pt-based nanocatalysts. It is impossible to cover all the recent research work about the hollow Pt-based nanocatalysts used in PEMFCs in this short review but we try to review most of the correlative literatures.

2. A brief overview of different Pt-based nanocatalysts in PEMFCs

Since platinum is a precious metal, most of the recent efforts have focused on not only reducing the amount of Pt but also enhancing catalytic activity and stability in the research of fuel cell. In the past several decades, significant effort has been put into the design and synthesis of different Pt-based nanostructured materials for PEMFC catalysts. The promising designs for Pt-based catalysts can be summarized as Pt-alloy catalysts, core–shell structured Pt-based catalysts, Pt-monolayer catalysts, Pt-based catalysts with high index, nanoporous Pt-based catalysts, hollow Pt-based nanocatalysts, and non-noble catalysts.

Pt alloyed with other non-noble metal named Pt-alloy catalysts is the common way to enhance the catalytic activity and reduce the quantum of noble Pt. Over the past decade, Pt-alloy catalysts used in PEMFC have been widely studied and reviewed [7–10]. The relation of structure, composition, and performance of the Pt-alloy nanocatalysts will be the pivotal direction in the following studies. Core-shell structured Pt-based nanocatalysts have attracted increasing attention due to their unique advantages in reducing Pt loading and improving the electrocatalytic activity [11,12]. Recently, Liu et al. [13] reviewed the development of the core–shell structured electrocatalysts used for low-temperature fuel cells. They thought the synthetical methods, characterization means, the relation of between the performance, structure and composition and so on are needed to optimize in the future studies. Among all kinds of different core–shell nanomaterials, core-Pt-monolayer structured catalysts have been regarded as one of the most efficient catalysts because of their high utilization of unit Pt. Pt monolayer on various core structures in an effort to stabilize Pt and Pt-group metals has been widely explored [14–21]. The obtained Pt-monolayer catalysts exhibited an outstanding activity for oxygen reduction reaction. The controlled synthesis method of Pt-monolayer catalysts and the influence of the core material are needed to optimize.

Nanoporous materials displayed many advantages in higher active surface area, controllable porosity and permeability, capillarity, and easy access of reactant to the electrode/electrolyte interface [22–24]. The Pt-based nanoporous catalysts have been regarded as one of the most promising catalysts used in PEMFC and explored widely in recent years. Nanoporous PtAu [25–27], PtNi [28–31], PtNiAl [32], PtCo [33], PtFe [34,35], PtCu [36], PtRuNi [37], Pt-based multimetallic alloy nanowires [38] catalysts and so on have been reported as cathode or anode catalysts used in PEMFC. However, the degree of porosity, the best composition, and well control over the Pt-based electrocatalyst nanostructure applied in PEMFC are very significant in the future studies.

Nanomaterials with high high-index planes, which have a large density of low-coordinated atoms situated on steps and kinks, have already been shown to exhibit exceptionally high electrocatalytic activity [39]. In order to increase the Pt utilization in the catalyst, Pt-based nanocatalysts with high high-index planes have been widely studied in recent years. Sun's group have successfully synthesized different Pt-based nanocatalysts with high-index planes and the obtained products shown a high electrocatalytic activity for the oxidation of CH_3OH, CH_3CH_2OH, CH_3COOH and son on [40–47]. Recently, Zhou et al. [48] reviewed the recent progress made in shape-controlled synthesis of metal nanocrystals with high-energy facets and open surface structure, including high-index facets and {110} facets, especially the electrochemically shape-controlled synthesis of Pt-group metal nanocrystals. The authors thought that size control, especially synthesis of nanocatalysts of high surface energy of several nanometers, was still a great challenge in this field.

The cost, performance and durability are three major criteria for the application of the PEMFC. Today, most PEMFC catalysts used are based on Pt nanomaterials, with the high price of this scarce precious metal having a decisive impact on costs. There are two approaches to reducing catalyst cost: one is to increase Pt utilization in the catalyst, and the other is to explore non-precious catalysts. The above mentioned Pt-alloyed nanocatalyst, M@Pt, Pt monolayer, hollow Pt, nanoporous Pt catalysts, and Pt-based nanocatalysts with high index are the widely used ways to increase Pt utilization in the catalysts. Different non-noble catalysts possibly used in PEMFC and the future research directions have been summarized and analyzed deeply in the recent review papers [49–55]. Despite extensive research work in finding non-Pt electrocatalysts, Pt-based nanocatalysts are still the most promising materials that can fulfill demands in fuel cells working in acid media.

3. Hollow Pt-based nanocatalysts

Hollow nanostructured metallic materials have been attracted by many researchers in recent years due to their new properties and potential applications based on their especial hollow structure. The synthesis, characterization and application of the hollow nanostructured materials have been reviewed for a general introduction to the field [56–60]. Recently, Lai et al. [61] reviewed the design and fabrication of complex spherical multi-shelled hollow structures as a replacement to simple hollow counterparts and their potential applications for dye-sensitized solar cells, fuel cells, Li-ion batteries, and supercapacitors. Here, our review will focus on the hollow pure Pt, Pt-based nanocatalysts and their applications in the PEMFCs.

3.1. Hollow pure Pt nanocatalysts

Liang et al. [62] firstly reported the synthesis of large-scale Pt hollow nanospheres at room temperature in a homogeneous solution by *in situ* galvanic replacement method with Co nanoparticles as sacrificial templates (see Fig. 1A). It was found that the centers of the spheres are brighter than the edges, which indicating the products have a hollow structure. Clear TEM and SEM images are the most powerful tools to prove the hollow structure. The obtained incomplete and porous shells of the Pt hollow nanospheres have a higher surface area and therefore exhibit enhanced electrocatalytic performance. Fig. 1B shows the cyclic voltammograms of Pt solid nanoclusters and hollow nanospheres on glass carbon electrode with a scan rate of 50 mV s^{-1}. The catalytic activity of the Pt hollow nanospheres is twice that of the solid Pt nanoclusters for the electrooxidation of CH_3OH in H_2SO_4 (0.5 M H_2SO_4 + 0.6 M CH_3OH). Recently, they extended the *in situ* galvanic replacement method to synthesize of Pt hollow nanostructures supported on graphene composites using Co nanoparticles grown onto graphene sheets as the sacrificial templates [63].

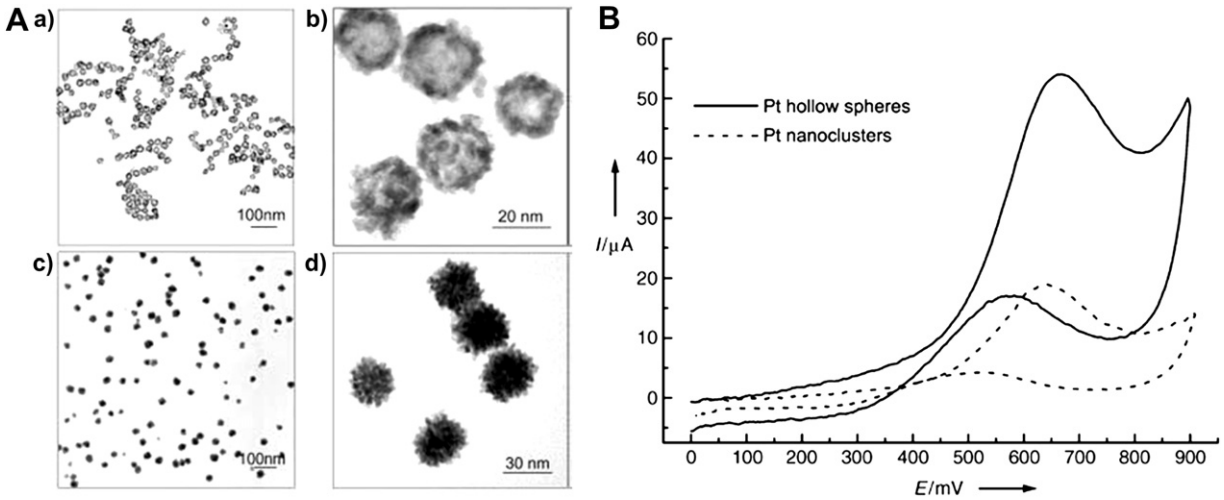

Fig. 1. A. TEM images of Pt hollow nanospheres (a) and (b), and solid nanoclusters (c) and (d). B. Cyclic voltammograms of Pt solid nanoclusters (dashed line) and hollow nanospheres (solid line) on a glass carbon electrode in 0.5 M H_2SO_4 + 0.6 M CH_3OH with a scan rate of 50 mV s^{-1}.

Later, Zhao et al. [64] reported the synthesis of carbon supported hollow Pt nanospheres employing cobalt metal nanoparticles as sacrificial templates. The carbon supported hollow Pt nanospheres exhibited enhanced electrocatalytic performance for methanol oxidation compared with carbon supported solid Pt nanoparticles, which can be explained by the higher active surface area of the carbon supported hollow Pt nanosphere. Then, Co nanoparticles were widely used as sacrificial templates to synthesize Pt-based hollow materials, which were applied to a signal-amplified electrochemical immunosensor [65], electrochemical immunosensor for human chorionic gonadotropin (HCG) assay [66], and electrochemical glucose biosensor [67].

Except for the Co nanoparticles, Ag nanoparticles are another kind common sacrificial template to synthesize Pt-based nanocatalyst with a hollow structure. Yang et al. [68] reported the synthesis of hollow Pt nanospheres by using bis(*p*-sulfonatophenyl) phenylphosphine (BSPP) to selectively remove the Ag cores of AgPt core–shell nanoparticles, which were obtained by the successive reduction method with a discontinuous Pt shell to allow the BSPP passage. The surface area per Pt hollow nanosphere is calculated to be approximately 1.52 times that of a corresponding solid particle. The authors attributed the higher specific activity of the Pt hollow nanospheres for the electrooxidation of CH_3OH in H_2SO_4 (0.5 M H_2SO_4 + 0.6 M CH_3OH) to the larger specific surface area prevalent in the porous hollow structure. Later, Tan et al. [69] reported the preparation of Pt hollow nanoboxes using Ag@Pt core–shell nanocubes as templates through the same method and studied the synthetical mechanism deeply. But, Kim et al. [70] reported another method to obtain hollow Pt nanospheres using Ag@Pt core–shell nanoparticles as the template. They found that that the core silver metal of a Ag@Pt core–shell polyhedral nanoparticle could be excavated by exciting the surface plasmon resonances of the shell platinum metal with laser pulses of 1064 nm and 30 ps, then a smooth hollow platinum nanosphere can be fabricated. The shape of the hollow Pt nanomaterials was based on the shape of the sacrificial templates. Bansal et al. [71] reported the synthesis of hollow Pt nanocubes by galvanic replacement approach using Ag nanocubes as the sacrificial templates. They investigated the hydrogen evolution reaction (HER) activity of Ag nanocubes replaced with different amounts of Pt, and demonstrate how the bimetallic composition significantly affects the activity of the alloyed nanomaterials. Recently, Pt hollow nanospheres, Pt nanotubes, and PtAu alloy nanotubes with controlled Pt:Au compositions are successfully prepared via a galvanic replacement process using sacrificial Ag templates [72]. The hollow Pt catalysts exhibited higher activities relative to the commercial Pt catalysts due to their hollow structures for formic acid electrooxidation. Among the monometallic hollow Pt catalysts, the Pt nanotubes exhibited better activity than the Pt hollow nanospheres due to their 1D structure.

After the reports of the hollow Pt nanospheres obtained in aqueous solution, Selvakannan et al. [73] have extended the galvanic replacement approach to organic solution. The hydrophobic spherical silver nanoparticles and hydrophobized $PtCl_6^{2-}$ ions may be carried out in an equally facile manner in organic solvents resulting in excellent hollow Pt nanoshells that are organically dispersible. The authors thought that the synthesis of hollow metal nanoparticles such as Pt in an organic environment would be of much greater value in catalytic applications than a water-based process.

Wang et al. [74] thought that Ni nanoparticles were suitable as templates because of their lower reduction potential and easily soluble in acid solution relative to Ag and Cu nanoparticles templates. Then they fabricated compact and smooth Pt hollow nanocrystals by galvanic replacement method using electrodeposited Ni nanoparticles on carbon powder as templates. The as-prepared hollow Pt nanocatalysts exhibited a sustained enhancement in Pt mass activity for oxygen reduction in acid fuel cells, which was attributed to the hollow-induced lattice contraction, high surface area per mass, and oxidation-resistant surface morphology. They concluded that the hollow nanoparticle affords larger particle size than a solid one with the same mass, thus significantly increasing the amount of the high-coordination surface sites, which were very important for enhancing the ORR activity and catalyst's stability.

Except for the galvanic replacement method using Co, Ag and Ni nanoparticles as the sacrificial templates, other methods and other different templates were found to synthesize Pt-based nanomaterials. For example, Hollow Pt nanoparticles were obtained through Kirkendall effect from Pt_3Co electrocatalyst reported by Dubau et al. [75]. They concluded that Co atoms can diffuse from the inner to the surface of Pt_3Co. When the cathode potential is above the onset of surface oxide formation, the decrease of the Co content is much faster over time, yielding to the formation of hollow Pt nanoparticles. Ataee-Esfahani et al. [76] developed a facile method to synthesize hollow Pt nanospheres with tunable nanosponge shell thicknesses by using silica particles

functionalized with amino group as templates. The maximum electrocatalytic activity for the methanol oxidation of the obtained hollow Pt nanospheres was around 1.7 times larger than that of commercially available Pt black. Such a unique Pt nanostructure effectively improved the electrocatalytic performance as Pt catalysts by facilitating the access of electroactive species to the whole Pt surface. Thiol-functionalized silica was also used as template to synthesize Ag, Au, Pd, Pt nanoparticles with a hollow structure [77]. Recently, monolayer ordered silica was used as template to synthesize ordered Pt and Pt/Ag hollow hemispheres by steric hindrance colloidal microspheres approach (SHCMA) through colloidal lithography and physical vapor deposition technology [78].

Minch et al. [79] have demonstrated a versatile and efficient electrochemical approach to prepare large area of on-substrate self-standing nanostructured hollow Pt and PtRu nanotubes using wet chemically processed ZnO nanotubes as a sacrificial template. Pt hollow capsules (from 250 to 400 nm) have been obtained by a spontaneous combustion reaction reported by Yang et al. [80]. In brief, Pt precursor ($[Pt(NH_3)_4]Cl_2$) was loaded on the surface of colloidal carbon spheres by wet-chemical impregnation. The resulting Pt composite supported on the carbon spheres combusted spontaneously when it was taken out of a cooled tube-furnace purged with argon and exposed to air at room temperature. Nanostructured Pt hollow capsules can be obtained after removal of the carbon spheres templates. Three kinds of Pt hollow particles were synthesized by pulsed-excimer-laser ablation method using different laser fluences (2.3–6.8 J cm^{-2}) and after 6000 laser shots reported by Yan et al. [81]. The authors propose that the hollow particles were formed on laser-produced bubbles which provided thermodynamically preferred nucleation sites and diffusion sinks for the laser-fabricated Pt clusters or particles. The hollow particles obtained could be beneficial for fundamental investigations and provide a new mechanistic approach to synthesize nanomaterials with a hollow structure. Pt micro/nanotubes and hollow Pt spheres were fabricated using a novel class of aromatic amide-based non-amphiphiles (organic template) that can self-assemble into vesicular and tubular structures by simply changing the solvents and/or concentrations [82]. Recently, Bai et al. explored a simple, clean, and economic method to synthesize hollow Pt nanotubes [83]. Well-defined Pt hollow nanotubes were synthesized through a templated photocatalytic method using zinc meso-tetra(4-pyridyl)porphyrin (ZnTPyP) as the template. The obtained Pt hollow nanotubes exhibited enhanced catalytic performance for methanol oxidation, which can be attributed to the porous nanostructured networks.

3.2. Hollow PtM nanocatalysts

It has been approved that Pt-based alloy catalysts exhibit enhanced catalytic activity and stability in PEMFCs than that of pure Pt catalyst [84]. Then, different kinds of hollow Pt-based PtM (M = Au, Ag, Co, Ni, Pb, Ru, Pd, Cu, Se) nanocatalysts have been reported by lots of researchers recently. Few ternary hollow Pt-based nanocatalysts were also studied.

3.2.1. PtAu

After successfully synthesis of Pt hollow nanospheres using Co nanoparticles as sacrificial templates, Liang et al. [85] extended this method to prepare PtAu bimetallic hollow tube-like 1-D nanomaterials and hollow nanospheres, which can be easily manipulated by only changing the concentration of citric acid.

Recently, PtAu alloy nanotubes with controlled Pt:Au compositions are successfully prepared via a galvanic replacement process using Ag nanotubes as the sacrificial templates [72]. The representative SEM, TEM images, EDS, and SAED patterns of the PtAu nanotubes are shown in Fig. 2A. The Pt_1Au_3 nanotubes catalyst was identified as the best electrocatalyst on the basis of its low onset potential, high catalytic activity, and high tolerance to CO poisoning than that of hollow Pt nanotubes for formic acid electrooxidation (see Fig. 2B). The enhanced electrochemical properties of the hollow AuPt nanotubes catalysts are most likely due to the ensemble effect and the electronic effects. Hollow and nanoporous PtAu alloy nanoparticles were reported by Lee et al. [86] using the same method and the products exhibited a high electrocatalytic activity for HCOOH oxidation.

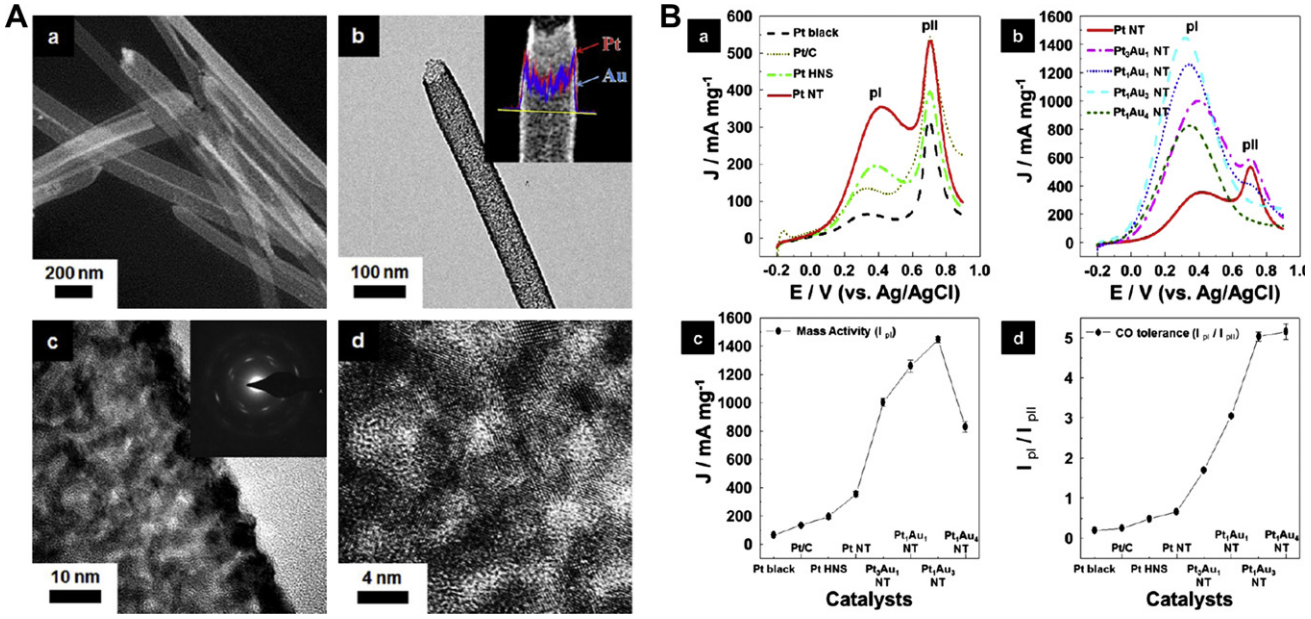

Fig. 2. A. (a) SEM (b) TEM, and (c), (d) HRTEM images of PtAu nanotubes. The insets of panels b and c show the EDS line scan and the SAED pattern of the PtAu nanotubes, respectively. B. Anodic polarization curves for HCOOH oxidation by (a) Pt black, Pt/C, hollow Pt nanoparticles (Pt HNS), hollow Pt nanotubes (Pt NT) and (b) the bimetallic hollow PtAu nanotubes (PtAu NT) with different compositions in a 0.5 M HCOOH + 0.5 M H_2SO_4 solution at a scan rate of 50 mV s^{-1}. The corresponding (c) mass activities and (d) CO-tolerance (I_{pI}/I_{pII}) of the catalysts given in panels a and b.

Functionalized TiO_2 and goethite were used as hard templates to synthesize hollow PtAu nanomaterials except for the *in situ* sacrificial templates method. Raspberry-like hierarchical PtAu nanoparticle assembling hollow spheres (RHAHS) with pore structure and complex morphology using NH_2-functionalized TiO_2 precursor as sacrificial template approach were reported by Guo et al. [87]. The authors considered that this method has some clear advantages including simplicity, quickness, high quality, good reproducibility, and no need of a complex post-treatment process (removing templates) and can be extended to other metal-based NP assembling hollow spheres. The as-prepared RHAHS exhibited more positive potential, higher specific activity, and higher mass activity for oxygen reduction reaction (ORR) than that of commercial platinum black (CPB) in 0.5 M H_2SO_4 solution. Liu et al. [88] constructed hollow and solid hierarchical paramecium-like AuPt bimetallic nanostructures in aqueous solution using goethite as environmentally friendly template via a seed-mediated growth process. Goethite plays the role of the *in situ* sacrificial template or the solid template depending on the experimental conditions. Both the hollow and solid hierarchical paramecium-like AuPt bimetallic nanostructures show good catalytic activities for the electron-transfer reaction between $Fe(CN)_6^{3-}$ and $S_2O_3^{2-}$ and may have promising applications in fuel cells, fine chemical synthesis, environmental monitoring and sensors.

3.2.2. PtAg

Bimetallic hollow AgPt nanoparticles with high Pt content were controlled synthesized by a successive reduction method through *in situ* formed Ag nanoparticles [89]. The authors found that the plasmon resonance peak locations corresponding to these bimetallic hollow particles could be tuned across the UV and visible spectrum region by controlling the Pt content, which makes these optically active nanostructures of great interest in both fundamental research and practical applications.

Later, hollow PtAg nanoparticles have been fabricated via the galvanic replacement of Ag nanospheres with Pt^{n+} [90]. As-prepared hollow PtAg nanocomposites can be transformed further into hollow Pt nanoparticles by removing residual silver with 0.5 M HNO_3. The catalytic ability of hollow PtAg nanocomposites was much more efficient than that of Ag nanospheres for the degradation reaction of rhodamine B in the presence of KBH_4.

Recently, distinct PtAg hollow nanostructures with controlled number of voids have been synthesized via galvanic replacement reaction using Ag nanocubes as the sacrificial template in the presence of HCl [91]. They obtained PtAg hollow nanoboxes, dimers, multimers, or popcorn-shaped nanostructures consisting of one, two, or multiple hollow domains (see Fig. 3A). The use of HCl allows the deposition of AgCl on the surface of Ag nanotubes to regulate the growth of Pt. These PtAg hollow nanomaterials exhibited high surface area and improved catalytic activity for methanol oxidation reaction because of the presence of large void space and porous walls (see Fig. 3B).

3.2.3. PtCo

While there are many reports of hollow sphere formation via galvanic replacement reactions, there are no examples where Co-based alloys form as the final products when Co nanoparticles are used as templates. Hollow PtCo alloy nanospheres synthesized through a novel galvanic replacement reaction that exploits an *in situ* nano-Co sacrificial template were reported by Vasque et al. [92]. From Fig. 4a, we can see that large hollow CoPt nanospheres with average diameters of 10–50 nm were obtained. The authors thought that the excess reducer $NaBH_4$ and appropriate protector (poly(vinylpyrrolidone)) (PVP) were the pivotal factors during the synthetical process. From the above analysis of the galvanic replacement reaction, we can see that this method is a promising approach to synthesize hollow alloy nanomaterials with controlled compositions. Actually, the galvanic replacement reaction has been applied to synthesize nanomaterials with different structure and composition. Later, one-dimensional (1D) hollow PtCo nanomaterials were synthesized using the same method and the

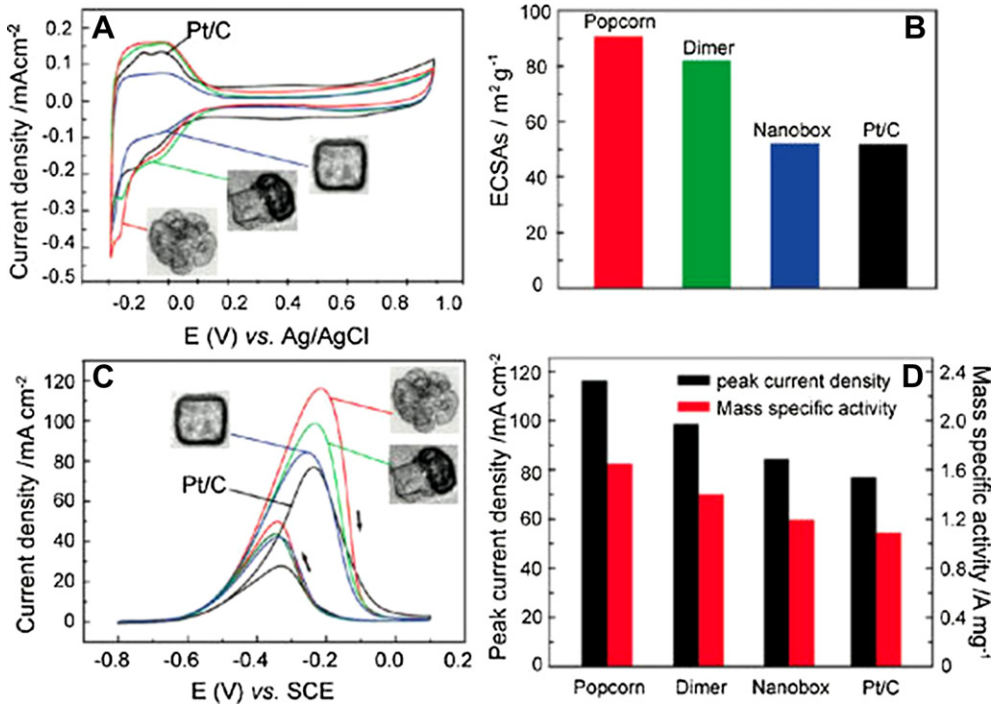

Fig. 3. (A) Cyclic voltammograms of Pt/C, Pt/Ag hollow nanoboxes, dimers, and popcorns in 1 M $HClO_4$. (B) Electrochemically activated surface areas (ECSA) of each catalyst. (C) CVs for methanol oxidation reactions (MOR) in a solution containing 1 M CH_3OH and 1 M KOH. (D) Mass activity of each catalyst. The scan rate for all CVs is 50 mV s^{-1}.

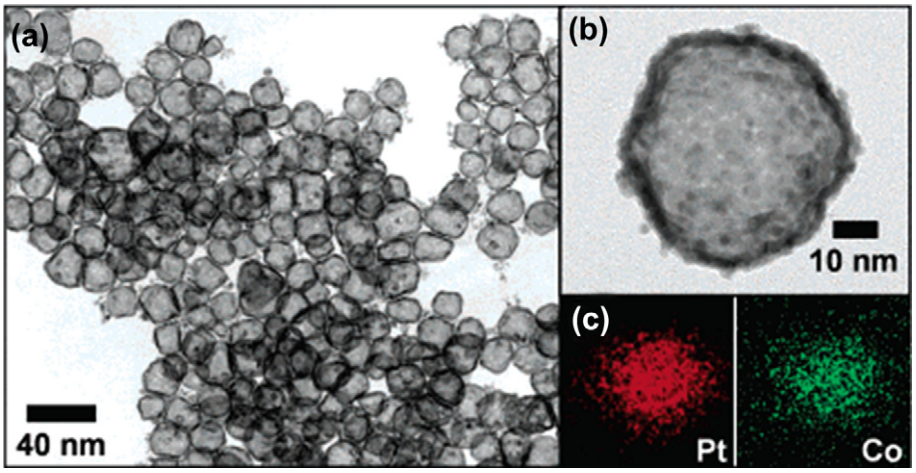

Fig. 4. TEM micrographs of (a) Pt Co hollow spheres and (b) a single hollow sphere (c) elemental mapping data (Co and Pt) for the sphere in (b).

products were transferred to an indium tin oxide (ITO) electrode surface simply realized via magnetic attraction [93]. The thus-prepared modified electrode was quite stable and displayed catalytic activity toward oxygen reduction reaction.

Based on the method mentioned above, we have synthesized PtCo chainlike nanocatalysts [94,95] (see Fig. 5a, b) and one-dimensional hollow PtCo nanospheres [96] (see Fig. 5c, d). The catalytic activity of the hollow PtCo chainlike nanocatalysts is much higher than that of the commercial Pt/C catalyst for the electro-oxidation of methanol in 0.1 M H_2SO_4. We concluded that the remarkably high activity of hollow PtCo chainlike nanocatalysts for oxidation of methanol may come from the special hollow structure,

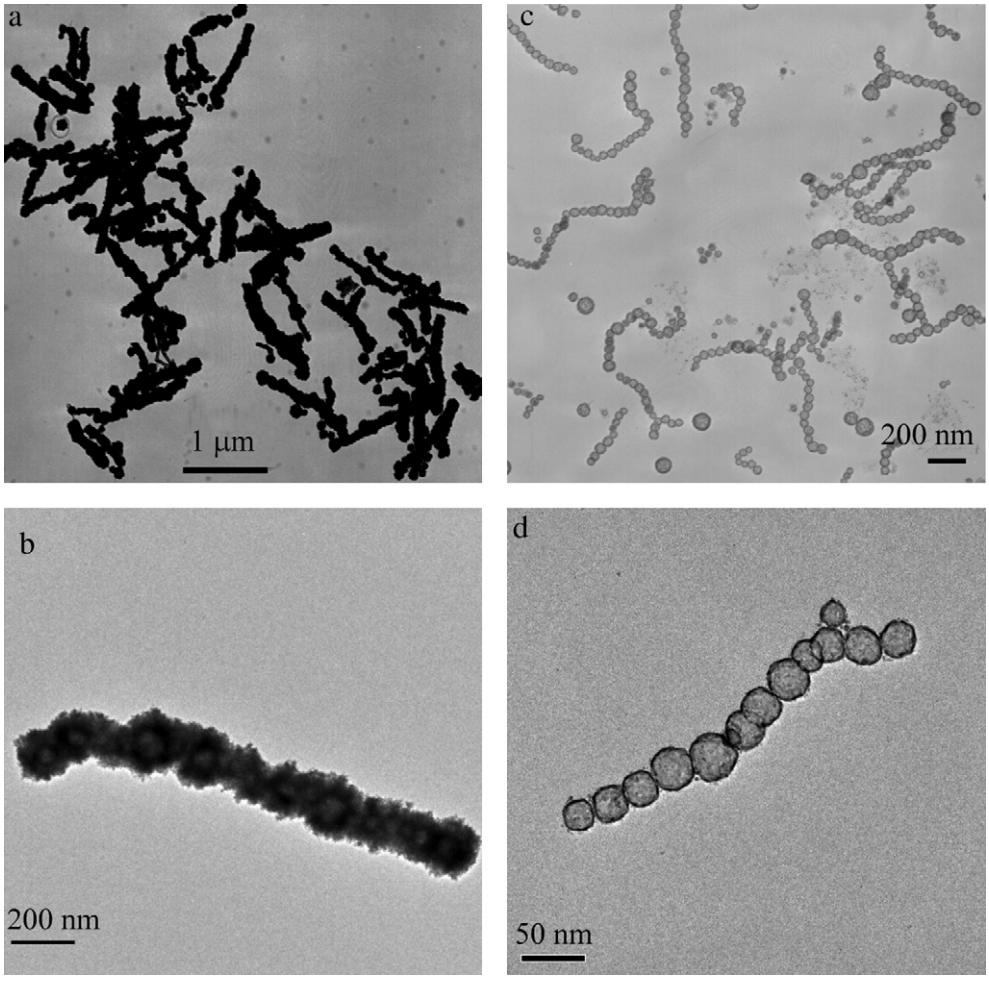

Fig. 5. Different magnification TEM images of one-dimensional CoPt nanorods (a) (b) and hollow CoPt chainlike nanocatalysts (c) (d).

the effect of the bimetallic function and the de-alloying process [97]. Then, PtCo hollow nanoparticles obtained by galvanic replacement reaction using Co nanoparticles as sacrificial templates were applied to electrochemical aptasensor [98].

Later, PtCo nanoparticles with a porous Co core and a shell of Pt tiny particles supported on a glassy carbon electrode (denoted as PtCo/GC) were prepared by galvanic replacement reaction between electrodeposited Co nanoparticles and K_2PtCl_6 solution [99]. The obtained PtCo/GC possesses a much higher catalytic activity toward CO and methanol electrooxidation than a nanoscale Pt thin film electrode in alkaline medium. They thought that the enhanced electrocatalytic activity may be attributed to the porous core–shell structure of PtCo nanoparticles, which provided more active sites and improved the property of CO-tolerance of PtCo due to the Co in the inner layer.

Recently, Sun et al. [100] reported the synthesis of well-aligned PtCo hollow nanochains through magnetic field-induced assembly approach combining with galvanic replacement using Co nanoparticles as sacrificial templates. The as-synthesized PtCo hollow chains can be well aligned by magnetic fields. Magnetic properties indicate that the shape anisotropy of 1D aligned nanochains plays a dominant role on their good controllable behavior. In the paper, they have extended the method to synthesize highly monodispersed hollow PtNi nanospheres successfully.

Other methods are also explored to synthesize hollow PtCo nanomaterials except for the galvanic replacement method using Co nanoparticles as sacrificial templates. PtCo hollow spheres with adjustable composition was synthesized via a very simple thermolytic reaction using anionic surfactant sodium dodecyl sulfate (SDS) as the capping and structure-directing agent in refluxing ethylene glycol [101]. The prepared PtCo hollow spheres demonstrated enhanced electrocatalytic activity for methanol oxidation compared with Pt and PtCo nanoparticles (0.5 M H_2SO_4 + 1.0 M CH_3OH) at the same Pt loading, which was attributed to changes in lattice structures or the electronic properties of the PtCo bimetal catalysts. The better electrocatalytic performance of hollow spheres could have been due to changes in lattice structures or the electronic properties of the PtCo bimetal by the authors.

3.2.4. PtNi

Nest-like hollow $Ni_{1-x}Pt_x$ spheres of submicrometer sizes have been prepared through a PSA-assisted (PSA = poly(styrene-co-methacrylic acid)) template method and the galvanic replacement reaction route [102]. The formation of $Ni_{1-x}Pt_x$ was attained through the replacement reaction between K_2PtCl_6 and Ni, which was first deposited on the surface of the PSA. After the partial consumption of Ni, the resultant $Ni_{1-x}Pt_x$-PSA core–shell structures are dispersed in a toluene solution to dissolve the PSA template cores, resulting in the formation of $Ni_{1-x}Pt_x$ hollow spheres. The obtained $Ni_{1-x}Pt_x$ alloy hollow spheres exhibit favorable catalytic activities for both the hydrolysis and the thermolysis of NH_3BH_3.

As predicted by Vasquez et al. [92], the galvanic replacement reaction has been applied to PtNi bimetallic systems. We have prepared hollow PtNi nanospheres (PtNi-a) and solid PtNi nanoparticles (PtNi-b) through galvanic replacement reaction and co-reduction method successfully [103]. Fig. 6A illustrates that large-scale hollow PtNi nanoparticles have been synthesized. It can be seen that the products are spherical and monodisperse with a diameter about 32 nm. The hollow PtNi nanospheres exhibit a superior electrocatalytic activity toward CH_3OH electrooxidation than that of commercial Pt/C catalyst and the solid PtNi nanoparticles in 0.1 M H_2SO_4 (see Fig. 6B). We concluded that the enhanced CH_3OH oxidation activity can be explained by bifunctional mechanism, the Pt electronic structure change and its especial hollow structure. Later, Hu et al. [104] reported the synthesis of grapheme-supported hollow PtNi nanocatalysts using the same method and the obtained catalysts shown a highly active electrooxidation for the methanol.

Carbon-supported PtNi alloy hollow nanoparticles with a narrow size distribution were synthesized by a one-step and one-pot synthetic approach without the need of surfactant and air-excluding condition [105]. In brief, carbon support was dispersed in an aqueous solution of $Pt(NH_3)_4Cl_2$ and $NiCl_2 \cdot 6H_2O$. Ethanol was added in order to increase the dispersion of the carbon support. To this mixture, an aqueous solution of $NaBH_4$ was added under vigorous magnetic stirring. After further stirring for 1 h, the resultant mixture was filtered and washed with a copious amount of triply distilled water, followed by drying at 100 °C for 24 h, to yield hollow PtNi/C catalysts. The obtained PtNi hollow nanoparticles showed excellent electrocatalytic performance for oxygen reduction reaction. One of the PtNi hollow nanoparticles exhibited a mass activity of 0.5 A per mg Pt, which exceeds the activity target of fuel cell catalysts (0.44 A per mg Pt). The enhanced oxygen reduction activity results partly from the geometry of the hollow structure. The authors gave a possible formation mechanism for the PtNi hollow nanoparticles, but how this simple process can lead to the formation of PtNi alloy hollow nanoparticles has not been fully elucidated in the paper.

3.2.5. PtPb

A non-intermetallic hollow PtPb/C catalyst was synthesized through a modified galvanic replacement reaction without using any surfactant and organometallic precursors, which were formed through the reaction between $PtCl_6^{2-}$ and metallic Pb [106] (see Fig. 7A). The hollow PtPb/C catalyst exhibited an activity as high as 3.6 times that of commercial Pd black and a much higher stability for electrooxidation of formic acid in 0.1 M H_2SO_4 (see Fig. 7B). The high electrocatalytic activity of the hollow PtPb/C for HCOOH oxidation was attributed to geometric effects and electronic effects between the Pt and Pb by the authors.

Recently, Li et al. [107] has successfully extended the galvanic replacement reaction to synthesize carbon supported hollow PdPb nanospheres using cobalt nanoparticles as sacrificial template. The current density of the hollow PdPb/C for the oxidation of HCOOH (0.5 M H_2SO_4+0.5 M HCOOH) is nearly 2.4 times of hollow Pd/C and 4.3 times of the solid Pd/C. The high catalytic activity is attributed to the combination of the advantage of hollow structure and the doping effect of Pb by the authors.

3.2.6. PtRu

Three-dimensional long range ordered hollow PtRu spheres were synthesized using three-dimensionally ordered macroporous carbon as a sacrificial template reported by Wang et al. [108]. The hollow Pt–Ru spheres obtained had a high BET surface area, high hydrogen adsorption stoichiometry (>0.5 H M^{-1}) and the size of the hollow spheres could be tailored using different sized porous carbon templates.

Hollow PtRu nanotubes were synthesized using wet chemically processed ZnO nanotubes as a sacrificial template reported by Minch et al. [79]. It is found that hollow PtRu nanotubes had better performance in comparison to pure hollow Pt nanotubes, but lower activity due to lesser number of Pt active sites.

Hollow Pt nanospheres (hPt) and ultrafine Ru nanoparticles were assembled based on electrostatic interactions to obtain hollow PtRu (hPtRu) assemblies [109]. The hollow Pt nanospheres were synthesized by galvanic replacement reaction using nanostructured Ag as the templates (see Fig. 8B). The routes of the assembly of hPt and Ru nanoparticles are shown in Fig. 8A. The hPtRu assemblies at a Pt:Ru molar ratio of 2:1 exhibit superior catalytic activity toward methanol oxidation in direct methanol fuel cells for

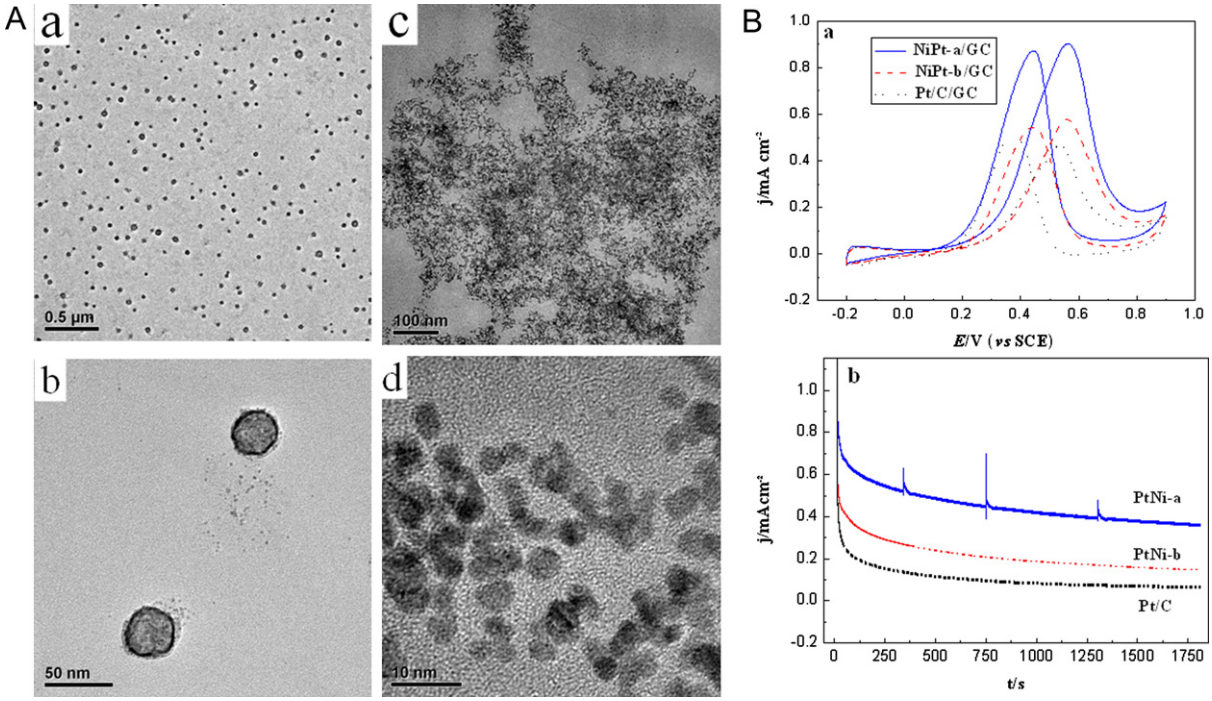

Fig. 6. A. TEM, high-magnification TEM images of hollow PtNi nanospheres (a, b) solid PtNi nanoparticles (c, d). B. (a) Cyclic voltammograms of PtNi-a, PtNi-b, and commercial Pt/C catalysts in 0.1 M H_2SO_4 + 0.1 M CH_3OH, (b) j–t curves obtained at 0.45 V with a scan rate of 50 mV s^{-1}.

the presence of a mixed-phase containing Pt and an effective oxophilic metal, and a smaller dilution effect on the Pt surface induced by Ru in the assemblies (see Fig. 8C).

3.2.7. PtPd

Hollow PtPd nanocrystals with different well-defined morphologies were synthesized by a galvanic replacement method using uniform Pd octahedral and cubic nanocrystals as sacrificial templates [110]. The synthetic parameters to produce various types of hollow PtPd bimetallic nanocrystals are illustrated in Fig. 9A. The obtained hollow PtPd alloy nanocrystals exhibited considerably enhanced oxygen reduction activities compared to those of core–shell Pd@Pt nanocrystals and commercial Pt/C catalyst, and their electrocatalytic activities were highly dependent on their morphologies (see Fig. 9C). The PtPd nanocages exhibited the largest improvement in oxygen reduction performance.

Hollow spherical PtPd/C catalyst has been prepared by microwave-assisted polyol process using sodium dodecyl sulfate as

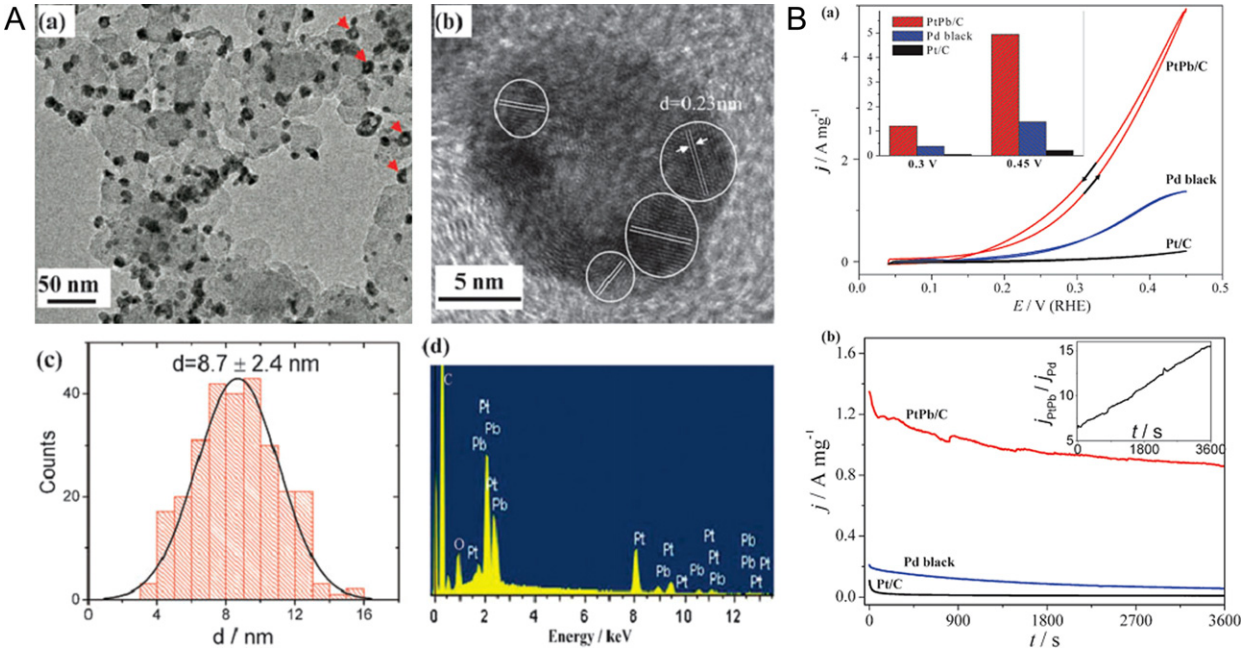

Fig. 7. A. (a) TEM, (b) HRTEM images, (c) histogram of particle size, and (d) EDX spectroscopy of hollow PtPb/C catalyst. B. (a) Cyclic voltammograms and (b) current–time curves recorded at 0.30 V (RHE), of HCOOH oxidation on PtPb/C, commercial Pd black and Pt/C catalysts in 0.5 M HCOOH + 0.1 M H_2SO_4. Inset in (a) shows the comparison of current recorded at 0.30 and 0.45 V. Inset in (b) shows the current ratio (j_{PtPb}/j_{Pd}) between PtPb/C and Pd black.

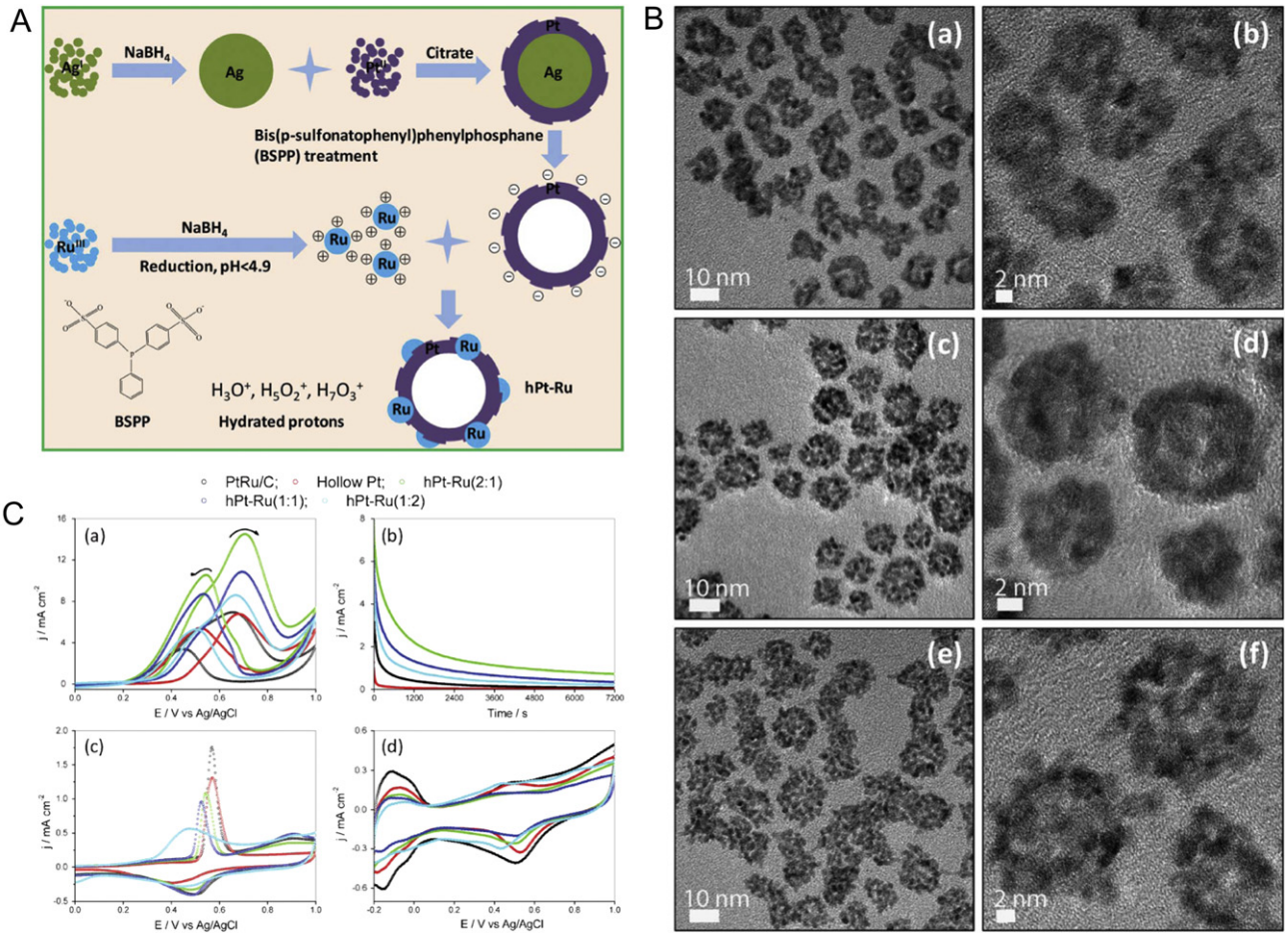

Fig. 8. A. Schematic illustration for the assembly of hPt and Ru nanoparticles. B. TEM (a, c, e) and HRTEM images (b, d, f) of hPtRu assemblies at Pt:Ru molar ratios of 2:1 (a, b), 1:1 (c, d), and 1:2 (e, f). C. (a) Cyclic voltammograms, and (b) chronoamperograms of commercial PtRu/C, hPt, and hPtRu assemblies at different Pt:Ru ratios in 0.1 M $HClO_4$ + 1 M CH_3OH. (c) Room-temperature CO stripping from the commercial PtRu/C, hPt, and hPtRu assemblies at different Pt:Ru ratios in 0.1 M $HClO_4$. (d) Cyclic voltammograms of commercial PtRu/C, hPt, and hPtRu assemblies at different Pt:Ru ratios in 0.1 M $HClO_4$ at room temperature.

a capping and structure-directing agent in ethylene glycol solution reported by Chu et al. [111]. The as-synthesized hollow PtPd/C catalyst exhibited enhanced electrocatalytic activity and stability toward methanol electrooxidation in comparison with the solid solution PtPd/C alloy and Pt/C catalysts because of the Pd-alloyed effect and their novel hollow spherical sandwich structure with open porosity and integrity.

3.2.8. PtCu

PtCu hollow nanocrystals were successfully prepared by the simultaneous reduction of K_2PtCl_6 and $Cu(acac)_2$ in the presence of oleylamine (OAm) and cetyltrimethylammonium bromide (CTAB) [112] (see Fig. 10B). In the galvanic replacement reaction between nano-Cu and K_2PtCl_6, the CTAB and OAm played an important role (see Fig. 10A). Cu^{2+} and Pt^{4+} exist in different materials and the addition of CTAB also has strong influence on the reaction rate of K_2PtCl_6. The contact of K_2PtCl_6 and OAm is weakened by the existence of CTAB. The specific activity for hollow PtCu catalyst is 2.08 mA cm^2. This value is much higher than 1.11 mA cm^2 for Pt black and 0.68 mA cm^2 for the Pt/C, which indicated that the PtCu hollow nanocrystals exhibited higher catalytic activity for methanol oxidation than commercial Pt black and Pt/C (see Fig. 10C).

Recently, hollow intermetallic $PtCu_3$ nanocages have been prepared through galvanic replacement mechanism between preformed Cu nanocrystals and Pt species in an organic solution system [113]. The method was also most the same to the ref. [103]. In brief, $H_2PtCl_6 \cdot 6H_2O$, [Cu-$(acac)_2$], and cetyltrimethylammonium bromide (CTAB) are dissolved in oleylamine (OAm). The resultant homogeneous solution is then solvothermally treated in a Teflon-lined stainless steel autoclave at 170 °C for 24 h. The as-prepared hollow $PtCu_3$ nanocages exhibit enhanced electrocatalytic activity for the methanol oxidation compared with solid $PtCu_3$ nanoparticles and a commercial Pt electrocatalyst (0.1 M $HClO_4$ + 1 M CH_3OH), which could be attributed to the unique hollow structure and possible synergetic effect of Pt and Cu components.

3.2.9. Other hollow Pt-based nanocatalysts

Except for the hollow Pt and PtM (M = Au, Ag, Co, Ni, Pb, Ru, Pd, Cu), other Pt-based nanomaterials with hollow structure were also studied. For example, PtSe hollow nanospheres with different coverages of Se were prepared using amorphous Se colloids as a sacrificial template [114]. The electrocatalytic activity of the PtSe hollow nanospheres for the oxidation of formic acid was better than that of hollow Pt and commercial Pt/C catalyst.

Hollow platinum–ruthenium–palladium (PtRuPd) spheres ternary alloy were prepared via a very simple soft-template method using tetrabutylammonium bromide (Bu_4NBr) as the template reported by Zhao et al. [115]. The PtRuPd hollow sphere catalyst showed a superior electrocatalytic activity toward the methanol oxidation reaction compared to the pure Pt and PtRuPd compact layers. The high catalytic of PtRuPd ternary hollow spheres toward

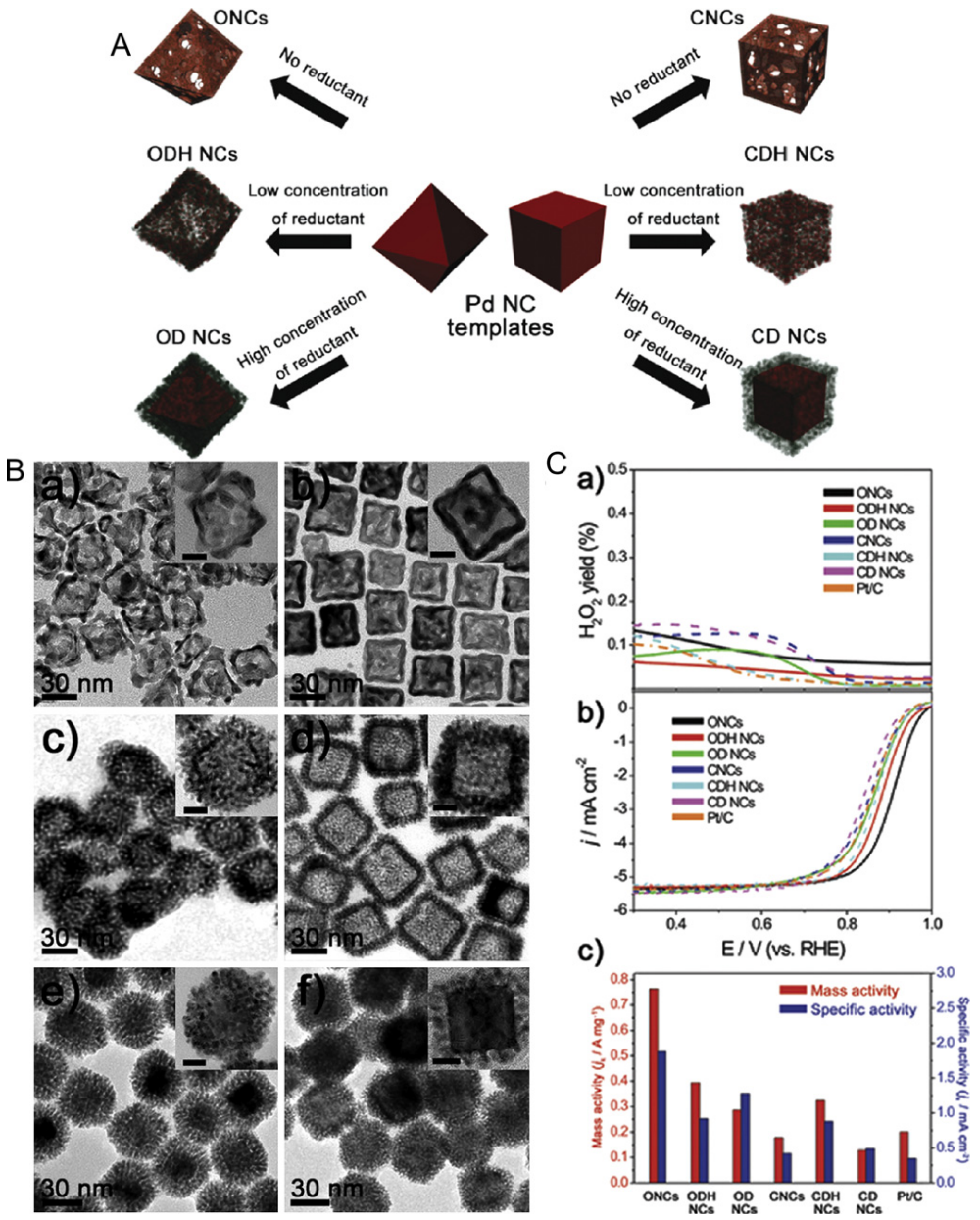

Fig. 9. A. Schematic illustration for the synthetic parameters to produce various types of PdPt bimetallic nanocrystals. B. TEM images of (a) ONCs, (b) CNCs, (c) ODH NCs, (d) CDH NCs, (e) OD NCs, and (f) CD NCs. High-magnification TEM images are shown in each inset. C. (a) H_2O_2 yield plots and (b) ORR polarization curves for the PdPt bimetallic NCs and Pt/C obtained using a RRDE in O_2-saturated 0.1 M $HClO_4$ at scan rate of 10 mV s^{-1} and a rotation rate of 1600 rpm. The ring potential was held at 1.2 V vs RHE. (c) Mass and area-specific activities at 0.85 V vs RHE for the various catalysts.

methanol can be ascribed to high specific area, Ru-assisted and Pd-assisted effects.

Recently, some new hollow Pt-based nanocrystals were reported. Hollow composite of Pt and $CoSn(OH)_6$ electrocatalysts supported on graphene nanosheets (HPt&$CoSn(OH)_6$/GNSs) were prepared using cobalt metal nanoparticles as sacrificial templates [116]. The as-prepared HPt&$CoSn(OH)_6$/GNSs exhibited improvement of electrooxidation activity for CH_3OH in comparison to solid composite of Pt and $CoSn(OH)_6$ catalyst supported on GNSs, pure Pt catalyst supported on GNSs, HPt&$CoSn(OH)_6$ supported on carbon black catalyst, and commercial E-tek PtRu/C catalyst. Hollow NiCo@Pt nanoalloy, in which a magnetic NiCo alloy hollow core is included in platinum nanoshells was prepared by the replacement between Ni or Co and $PtCl_6^{2-}$ by employing NiCo nanoicosahedrons as a sacrificial template in the presence of citrate acid reported by Wen et al. [117]. The as-obtained NiCo@Pt hollow nanospheres exhibited excellent enhancement of visible-light-driven photocatalysis activity for nano-ZnO toward methyl blue (MB) solution not only under UV-light but also under UV-filtered light.

Except for the Pt-based nanostructured materials, hollow Au [118], AuAg [119–121], Pd [122–124], PdPb [107], PdAu [125,126], PdRh [127], PdCu [128], PdCe [129], PdAg [130–132], PdFe [133] nanomaterials and so on have also been studied widely. Among them, hollow Pd, PdAu, PdRh, PdPb, and PdCu nanomaterials were widely applied as anode or cathode catalysts for fuel cell, especially for the direct formic acid fuel cells (DFAFCs). Hollow Pd-based nanocatalysts used in DFAFCs will be reviewed in another paper.

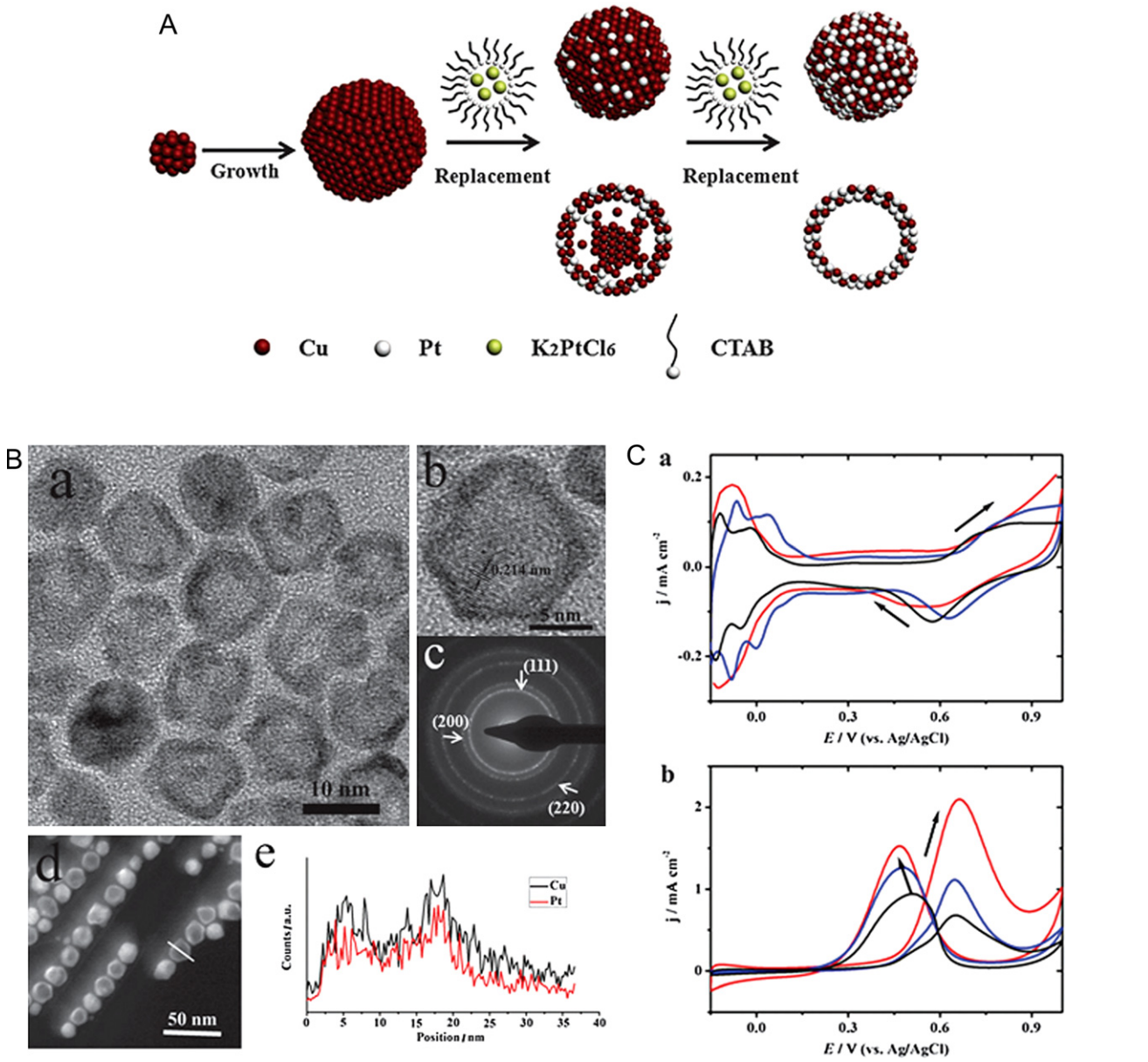

Fig. 10. A. Schematic illustration of the formation. B. (a) TEM, (b) HRTEM images, (c) SAED patterns, (d) representative HAADF-STEM image, (e) line-scanning profile across PtCu hollow nanospheres. C. (a) CVs of PtCu hollow nanocrystals (red), Pt/C (black) and Pt black (blue) in 0.5 M H_2SO_4, (b) CVs of methanol oxidation on PtCu hollow nanocrystals (red), Pt/C (black) and Pt black (blue) in 0.5 M H_2SO_4 + 1 M CH_3OH. Arrows indicate the potential scan direction. Scan rate: 50 mV s^{-1}. (For interpretation of the references to color in this figure legend, the reader is referred to the web version of this article.)

3.3. Summarization of hollow Pt-based nanocatalysts

Hollow Pt-based and Pd-based nanostructured materials are the promising candidates applied in the PEFMCs because of their especial hollow structure and have been studied widely in recent years. The catalytic performance highly depends on the compositions, size and surface structure of these hollow catalysts. Then, syntheses yielding hollow Pt and Pd-based nanocatalysts with controllable shape, size and composition are crucial for progress in this field.

Hollow nanoparticles were usually synthesized through a hard template-mediated method. This method is based on the use of an appropriate template material, on which will be coated with the metal layer of the cage. The inside template is etched away and an empty metallic nanocage is formed. For the above hollow Pt-based nanocatalyst, nano-Ag [68–70], SiO_2 [76], TiO_2 [87], ZnO [79], goethite [88] and carbon spheres [108] are used as the hard templates. Other soft templates such as tetrabutylammonium bromide [115,129] and organic template [82] are also used to synthesize hollow Pt-based nanomaterials. This template-mediated method consists of the removal of the template after the synthesis, which may destroy the structure of the products. Today, the most common method used for the synthesis of the hollow Pt-based nanocatalysts is the galvanic replacement method. Galvanic replacement method (GRM) is a special template method, in which one substance is served as a suitable sacrificial template and reacts with other appropriate metal ions according to their different standard reduction potentials, resulting in the formation of excellent hollow particles that take on the shape of the sacrificial template [96]. This method was developed by Sun and Xia [134] and was firstly

extended to synthesize Pt-based catalysts used in fuel cell by Bai et al. [62]. Different nanostructured Co [62–67,84,92–100,107,117–125], Ag [71–73,89–91,122,132], Ni [74,103,104], Cu [112,113,127], Pb [106], Pd [110] particles, especially the Co nanoparticles, are used as sacrificial templates widely to prepare hollow Pt-based and Pd-based nanocatalysts. Except for the common template-mediated method and galvanic replacement method, researchers have explored some new methods including nanoscale Kirkendall effect [28,75], spontaneous combustion reaction [80], pulsed-excimer-laser ablation method [81], thermolytic reaction [102], one-pot synthetic approach [105], microwave-assisted polyol process [111], electrochemical method [126], solvothermal method [130], and vesicle-assisted chemical reduction method [133] to synthesize hollow Pt-based nanocatalysts.

From the above summarization we can see that galvanic replacement method was the widely used method to synthesize different Pt-based nanocatalysts with a hollow structure. The advantages of the galvanic replacement method can be concluded as the following aspects: (1) the reaction mechanism is simple. Once two substances have different standard reduction potentials (SRP), they can react with each other. So lots of nanoparticles with low standard reduction potential are all the underlying sacrificial templates, especially the particles with well-controlled size and shape. (2) The framework of the final products can be well controlled through varying the reaction conditions such as the ratio of raw material, the quantity of the reducer and so on. We can obtain core–shell including monolayer [14–21], solid [135,136] or hollow Pt-based nanocatalysts which have been summarized in our review. (3) The final composition of the products can be adjusted easily. For example, when Co sacrificial template was consumed completely, we can obtain hollow Pt nanoparticles [62–67,75] without Co element. When the Co sacrificial template was reacted partly or followed with a co-reduction process, we can obtain hollow CoPt nanocatalysts [92–99] including Co element. (4) The shape of the final products can be well controlled based on the shape of the sacrificial template. Then the products with different shapes including sphere [62–71], cube [91], tube [72], chain [93–100], polyhedron [110] and so on can be synthesized through galvanic replacement method. (5) This method can be modified or combined with other methods to adjust the products we needed. For example, in ref. [109], as shown in Fig. 8, galvanic replacement method and electrostatic interactions were combined together to synthesize the assembly composing of hollow Pt nanospheres and ultrafine Ru nanoparticles. In the future research about the hollow Pt-based nanocatalysts, the galvanic replacement method is still the most prospective and challenging method. Finding facile and appropriate sacrificial template with low standard reduction potential and controllable shape and size will be the key in the development of this method. Modified GRE or GRE combined with other methods were another important direction in this field. Some new method such as electrochemical and solvothermal method are deserved.

4. Conclusions

In conclusion, we have summarized the recent progress in the field of preparation of hollow Pt-based nanocatalysts and their applications in PEMFCs. The hollow Pt-based nanostructured catalysts can be synthesized through different methods, in which the galvanic replacement method is the most prospective and challenging method and will be extended to other system widely. The electrochemical and solvothermal methods are latent methods to synthesize hollow nanostructured materials.

Future work should focus on the following aspects: (1) exploring new controllable sacrificial templates with well-controlled shape and size to synthesize hollow controlled Pt-based and Pd-based nanocatalysts application in PEMFCs through galvanic replacement method or modified GRE or method combined with GRE. (2) Developing new methods with high-speed, large-scale and low-cost to synthesize hollow Pt-based nanocatalysts. (3) Validating the activity and stability of these hollow Pt-based catalysts using real fuel cell operating conditions to utilize the advantages of the hollow structures completely. (4) Optimizing the synthetical strategies to make the Pt-based nanocatalyst into the each cavum of the hollow support. (5) Exploring the possibility of hybrids using hollow Pt-based nanocatalysts supported in the hollow support as catalysts applied in PEMFCs. It is clear that a more intensive research effort will be put on the development of hollow precious metal-based nanomaterials including the Pt-based nanocatalysts applied in the PEMFCs.

References

[1] A.B. Stambouli, Renew. Sust. Energ. Rev. 15 (2011) 4507–4520.
[2] V. Mthta, J.S. Cooper, J. Power Sources 114 (2003) 32–53.
[3] S.M. Haile, Acta Mater. 51 (2003) 5981–6000.
[4] M.K. Debe, Nature 486 (2012) 43–51.
[5] H. Liu, J. Qu, Y. Chen, J. Li, F. Ye, J.Y. Lee, J. Yang, J. Am. Chem. Soc. 134 (2012) 11602–11610.
[6] M.A. Mahmoud, M.A. El-Sayed, Langmuir 28 (2012) 4051–4059.
[7] H. Liu, C. Song, L. Zhang, J. Zhang, H. Wang, D.P. Wilkinson, J. Power Sources 155 (2006) 95–110.
[8] A. Chen, P. Holt-Hindle, Chem. Rev. 110 (2010) 3767–3804.
[9] Y. Bing, H. Liu, L. Zhang, D. Ghosh, J. Zhang, Chem. Soc. Rev. 39 (2010) 2184–2202.
[10] C. Wang, N.M. Markovic, V.R. Stamenkovic, ACS Catal. 2 (2012) 891–898.
[11] C.R. Ghosh, P. Santanu, Chem. Rev. 112 (2012) 2373–2433.
[12] H. Zhang, C. Cao, J. Zhao, R. Liu, J. Ma, Chin. J. Catal. 33 (2012) 222–229.
[13] B. Liu, S. Liao, Z. Liang, Prog. Chem. 23 (2011) 852–859.
[14] R.R. Adzic, J. Zhang, K. Sasaki, M.B. Vukmirovic, M. Shao, J.X. Wang, A.U. Nilekar, M. Mavrikakis, J.A. Valerio, F. Uribe, Top. Catal. 46 (2007) 249–262.
[15] K. Sasaki, H. Naohara, Y. Cai, Y.M. Choi, P. Liu, M.B. Vukmirovic, J.X. Wang, R.R. Adzic, Angew. Chem. Int. Ed. 49 (2010) 8602–8607.
[16] T. Ghosh, M. Vukmirovic, F. DiSalvo, R.R. Adzic, J. Am. Chem. Soc. 132 (2010) 906–907.
[17] K.A. Kuttiyiel, K. Sasaki, Y.M. Choi, D. Su, P. Liu, R.R. Adzic, Energy Environ. Sci. 5 (2012) 5297–5304.
[18] S. Papadimitriou, S. Armyanov, E. Valova, A. Hubin, O. Steenhaut, E. Pavlidou, G. Kokkinidis, S. Sotiropoulos, J. Phys. Chem. C 114 (2010) 5217–5223.
[19] B.I. Podlovchenko, V.A. Krivchenko, Yu. M. Maksimov, T.D. Gladysheva, L.V. Yashina, S.A. Evlashin, A.A. Pilevsky, Electrochim. Acta 76 (2012) 137–144.
[20] B.I. Podlovchenko, U.E. Zhumaev, Yu. M. Maksimov, J. Electroanal. Chem. 651 (2011) 30–37.
[21] A. Tegoua, S. Papadimitrioua, I. Mintsouli, S. Armyanov, E. Valova, G. Kokkinidis, S. Sotiropoulos, Catal. Today 170 (2011) 126–133.
[22] E.A. Anumol, A. Halder, C. Nethravathi, B. Viswanath, N. Ravishankar, J. Mater. Chem. 21 (2011) 8721–8726.
[23] N. Menzel, E. Ortel, R. Kraehnert, P. Strasser, ChemPhysChem 13 (2012) 1385–1394.
[24] W. Yuan, Y. Tang, X. Yang, Z. Wan, Appl. Energ. 94 (2012) 309–329.
[25] J. Xu, C. Zhang, X. Wang, H. Ji, C. Zhao, Y. Wang, Z. Zhang, Green Chem. 13 (2011) 1914–1922.
[26] Z. Zhang, Y. Wang, X. Wang, Nanoscale 3 (2011) 1663–1674.
[27] D.A. McCurry, M. Kamundi, M. Fayette, F. Wafula, N. Dimitrov, ACS Appl. Mater. Interfaces 3 (2011) 4459–4468.
[28] D. Wang, P. Zhao, Y. Li, Scientific Rep. 37 (2011) 1–5.
[29] J. Snyder, I. McCue, K. Livi, J. Erlebacher, J. Am. Chem. Soc. 134 (2012) 8633–8645.
[30] C. Zhou, X. Wang, X. Jia, H. Wang, C. Liu, Y. Yang, Electrochem. Commun. 18 (2012) 33–36.
[31] L.X. Ding, A.L. Wang, G.R. Li, Z.Q. Liu, W.X. Zhao, C.Y. Su, Y.X. Tong, J. Am. Chem. Soc. 134 (2012) 5730–5733.
[32] R. Wang, C. Xu, X. Bi, Y. Ding, Energy Environ. Sci. 5 (2012) 5281–5286.
[33] H. Qiu, F. Zou, ACS Appl. Mater. Interfaces 4 (2012) 1404–1410.
[34] H. Qiu, X. Huang, J. Mater. Chem. 22 (2012) 7602–7608.
[35] C. Xu, Q. Li, Y. Liu, J. Wang, H. Geng, Langmuir 28 (2012) 1886–1892.
[36] C. Xu, Y. Liu, J. Wang, H. Geng, H. Qiu, ACS Appl. Mater. Interfaces 3 (2011) 4626–4632.
[37] W. Wang, R. Wang, H. Wang, S. Ji, J. Key, X. Li, Z. Lei, J. Power Sources 196 (2011) 9346–9351.
[38] L. Liu, Z. Huang, D. Wang, R. Scholz, E. Pippel, Nanotechnology 22 (2011) 105604–105609.
[39] N. Tian, Z.Y. Zhou, S.G. Sun, J. Phys. Chem. C 112 (2008) 19801–19817.
[40] N. Tian, Z.Y. Zhou, S.G. Sun, Y. Ding, Z.L. Wang, Science 316 (2007) 732–735.

[41] Z.Y. Zhou, N. Tian, Z.Z. Huang, D.J. Chen, S.G. Sun, Faraday Discuss. 140 (2008) 81–92.
[42] Z.Y. Zhou, Z.Z. Huang, D.J. Chen, Q. Wang, N. Tian, S.G. Sun, Angew. Chem. Int. Ed. 49 (2010) 411–414.
[43] Q.S. Chen, Z.Y. Zhou, F.J. Vidal-Iglesias, J. Solla-Gullón, J.M. Feliu, S.G. Sun, J. Am. Chem. Soc. 133 (2011) 12930–12933.
[44] Y.J. Deng, N. Tian, Z.Y. Zhou, R. Huang, Z.L. Liu, J. Xiao, S.G. Sun, Chem. Sci. 3 (2012) 1157–1161.
[45] Z.Y. Zhou, S.J. Shang, N. Tian, B.H. Wu, N.F. Zheng, B.B. Xu, C. Chen, H.H. Wang, D.M. Xiang, S.G. Sun, Electrochem. Commun. 22 (2012) 61–64.
[46] L. Wei, Y.J. Fan, N. Tian, Z.Y. Zhou, X.Q. Zhao, B.W. Mao, S.G. Sun, J. Phys. Chem. C 116 (2012) 2040–2044.
[47] H.X. Liu, N. Tian, M.P. Brandon, Z.Y. Zhou, J.L. Lin, C. Hardacre, W.F. Lin, S.G. Sun, ACS Catal. 2 (2012) 708–715.
[48] Z.Y. Zhou, N. Tian, J.T. Li, I. Broadwell, S.G. Sun, Chem. Soc. Rev. 39 (2011) 4167–4185.
[49] L. Zhang, J.J. Zhang, D.P. Wilkinson, H.J. Wang, J. Power Sources 156 (2006) 171–182;
Z. Chen, D. Higgins, A. Yu, L. Zhang, J. Zhang, Energy Environ. Sci. 4 (2011) 3167–3192.
[50] C.W.B. Bezerra, L. Zhang, K. Lee, H. Liu, A.L.B. Marques, E.P. Marques, H. Wang, J. Zhang, Electrochim. Acta 53 (2008) 4937–4951.
[51] E. Antolini, E.R. Gonzalez, Appl. Catal. B 96 (2010) 245–266.
[52] A. Ishihara, Y. Ohgi, K. Matsuzawa, S. Mitsushima, K. Ota, Electrochim. Acta 55 (2010) 8005–8012.
[53] A.A. Gewirth, M.S. Thorum, Inorg. Chem. 49 (2010) 3557–3566.
[54] A. Brouzgou, S.Q. Song, P. Tsiakaras, Appl. Catal. B: Environ. 127 (2012) 371–388.
[55] R. Othman, A.L. Dicks, Z. Zhu, Int. J. Hydrogen Energ. 37 (2012) 357–372.
[56] Y. Sun, B. Mayers, Y. Xia, Adv. Mater. 15 (2003) 641–646.
[57] J. Han, G. Song, R. Guo, Adv. Mater. 18 (2006) 3140–3144.
[58] A.J. Wang, Y.P. Lu, R.X. Sun, Mat. Sci. Eng. A 460–461 (2007) 1–6.
[59] H.J. Fan, U. Gösele, M. Zacharias, Small 3 (2007) 1660–1671.
[60] H.C. Zeng, J. Mater. Chem. 21 (2011) 7511–7526.
[61] X. Lai, J.E. Halperta, D. Wang, Energy Environ. Sci. 5 (2012) 5604–5618.
[62] H.P. Liang, H.M. Zhang, J.S. Hu, Y.G. Guo, L.J. Wan, C.L. Bai, Angew. Chem. Int. Ed. 43 (2004) 1540–1543.
[63] Y.P. Xiao, S. Wan, X. Zhang, J.S. Hu, Z.D. Wei, L.J. Wan, Chem. Commun. 48 (2012) 10331–10333.
[64] J. Zhao, W. Chen, Y. Zheng, X. Li, J. Power Sources 162 (2006) 168–172.
[65] H. Liu, R. Yu, K. Peng, H. Zhao, L. Li, X. Wu, Electroanal. 22 (2010) 2577–2586.
[66] H. Yang, R. Yuan, Y. Chai, Y. Zhuo, H. Su, J. Chem. Technol. Biotechnol. 85 (2010) 577–582.
[67] Y. Wang, R. Yuan, Y. Chai, W. Li, Y. Zhuo, Y. Yuan, J. Li, J. Mol. Catal. B: Enzym. 71 (2011) 146–151.
[68] J. Yang, J.Y. Lee, H.P. Too, S. Valiyaveettil, J. Phys. Chem. B 110 (2006) 125–129.
[69] Y.N. Tan, J. Yang, J.Y. Lee, D.I.C. Wang, J. Phys. Chem. C 111 (2007) 14084–14090.
[70] S.J. Kim, C.S. Ah, D.J. Jang, Adv. Mater. 19 (2007) 1064–1068.
[71] V. Bansal, A.P. O'Mullane, S.K. Bhargava, Electrochem. Commun. 11 (2009) 1639–1642.
[72] Y. Kim, H.J. Kim, Y.S. Kim, S.M. Choi, M.H. Seo, W.B. Kim, J. Phys. Chem. C 116 (2012) 18093–18100.
[73] P.R. Selvakannan, M. Sastry, Chem. Commun. (2005) 1684–1686.
[74] J.X. Wang, C. Ma, Y.M. Choi, D. Su, Y. Zhu, P. Liu, R. Si, M.B. Vukmirovic, Y. Zhang, R.R. Adzic, J. Am. Chem. Soc. 133 (2011) 13551–13557.
[75] L. Dubau, J. Durst, F. Maillard, L. Guétaz, M. Chatnnet, J. André, E. Rosssinot, Electrochim. Acta 56 (2011) 10658–10677.
[76] H. Ataee-Esfahani, Y. Nemoto, L. Wang, Y. Yamauchi, Chem. Commun. 47 (2011) 3885–3887.
[77] J.H. Park, Y.G. Lee, S.G. Oh, J. Ceram. Process. Res. 12 (2011) 456–461.
[78] Z. Chen, J. Fu, Q. Xu, Y. Guo, H. Zhang, J. Chen, J. Zhang, G. Tian, B. Yang, J. Colloid Interf. Sci. 391 (2013) 54–59.
[79] R. Minch, M. Es-Souni, Chem. Commun. 47 (2011) 6284–6286.
[80] R. Yang, H. Li, X. Qiu, L. Chen, Chem. Eur. J. 12 (2006) 4083–4090.
[81] Z. Yan, R. Bao, D.B. Chrisey, Nanotechnology 21 (2010) 145609–145616.
[82] Y.X. Xu, G.T. Wang, X. Zhao, X.K. .Jiang, Z.T. Li, Soft Matter 6 (2010) 1246–1252.
[83] F. Bai, Z. Sun, H. Wu, R.E. Haddad, X. Xiao, H. Fan, Nano Lett. 11 (2011) 3759–3762.
[84] O.A. Petrii, J. Solid State Electrochem. 12 (2008) 609–642.
[85] H.P. Liang, Y.G. Guo, H.M. Zhang, J.S. Hu, L.J. Wan, C.L. Bai, Chem. Commun. (2004) 1496–1497.
[86] D. Lee, H.Y. Jiang, S. Hong, S. Park, J. Colloid Interf. Sci. 388 (2012) 74–79.
[87] S. Guo, S. Dong, E. Wang, J. Phys. Chem. C 113 (2009) 5485–5492.
[88] W. Liu, E. Repo, M. Heikkilä, M. Leskelä, M. Sillanpää, Nanotechnology 21 (2010) 395604–395613.
[89] J. Gao, X. Ren, D. Chen, F. Tang, J. Ren, Scripta Mater. 57 (2007) 687–690.
[90] M.R. Kim, D.K. Lee, D.J. Jang, Appl. Catal. B: Environ. 103 (2011) 253–260.
[91] W. Zhang, J. Yang, X. Lu, ACS Nano 6 (2012) 7397–7405.
[92] Y. Vasque, A.K. Sra, R.E. Schaak, J. Am. Chem. Soc. 127 (2005) 12504–12505.
[93] J.F. Zhai, M.H. Huang, Y.M. Zhai, S.J. Dong, J. Mater. Chem. 18 (2008) 923–928.
[94] X.W. Zhou, Q.S. Chen, Z.Y. Zhou, S.G. Sun, J. Nanosci. Nanotechnol. 9 (2009) 2392–2397.
[95] X.W. Zhou, R.H. Zhang, S.G. Sun, Acta Phys.-Chim. Sin. 26 (12) (2010) 3360–3364.
[96] X.W. Zhou, R.H. Zhang, D.M. Zeng, S.G. Sun, J. Solid State Chem. 183 (2010) 1340–1346.
[97] X.W. Zhou, Y.L. Gan, S.G. Sun, Acta Phys.-Chim. Sin. 28 (9) (2012) 2071–2076.
[98] K. Peng, H. Zhao, X. Wua, Y. Yuan, R. Yuan, Sensors Actuat. B 169 (2012) 88–95.
[99] Q.S. Chen, S.G. Sun, Z.Y. Zhou, Y.X. Chen, S.B. Deng, Phys. Chem. Chem. Phys. 10 (2008) 3645–3654.
[100] Q. Sun, Wang, R. Wang, J. Phys. Chem. C 116 (2012) 5352–5357.
[101] G. Chen, D. Xia, Z. Nie, Z. Wang, L. Wang, L. Zhang, J. Zhang, Chem. Mater. 19 (2007) 1840–1844.
[102] F. Cheng, H. Ma, Y. Li, J. Chen, Inorg. Chem. 46 (2007) 788–794.
[103] X.W. Zhou, R.H. Chen, Z.Y. Zhou, S.G. Sun, J. Power Sources 196 (2011) 5844–5848.
[104] Y. Hu, P. Wu, H. Zhang, C. Cai, Electrochim. Acta 85 (2012) 314–321.
[105] S.J. Bae, S.J. Yoo, Y. Lim, S. Kim, Y. Lim, J. Choi, K.S. Nahm, S.J. Hwang, T.H. Lim, S.K. Kim, P. Kim, J. Mater. Chem. 22 (2012) 8820–8825.
[106] D.J. Chen, Z.Y. Zhou, Q. Wang, D.M. Xiang, N. Tian, S.G. Sun, Chem. Commun. 46 (2010) 4252–4254.
[107] R. Li, H. Hao, W.B. Cai, T. Huang, A. Yu, Electrochem. Commun. 12 (2012) 901–904.
[108] H. Wang, Y.W. Li, S.J. Cho, X.D. Li, D.P. Kim, Micropor. Mesopor. Mat. 117 (2009) 208–212.
[109] F. Ye, J. Yang, W. Hu, H. Liu, S. Liao, J. Zeng, J. Yang, RSC Adv. 2 (2012) 7479–7486.
[110] J.W. Hong, S.W. Kang, B.S. Choi, D. Kim, S.B. Lee, S.W. Han, ACS Nano 6 (2012) 2410–2419.
[111] Y.Y. Chu, Z.B. Wang, Z.Z. Jiang, D.M. Gu, G.P. Yin, J. Power Sources 203 (2012) 17–25.
[112] X. Yu, D. Wang, Q. Peng, Y. Li, Chem. Commun. 47 (2011) 8094–8096.
[113] B.Y. Xia, H.B. Wu, X. Wang, X.W. Lou, J. Am. Chem. Soc. 134 (2012) 13934–13937.
[114] L.L. Yan, Q.N. Jiang, D.Y. Liu, Y. Zhong, F.P. Wen, X.C. Deng, Q.L. Zhong, B. Ren, Z.Q. Tian, Acta Phys.-Chim. Sin. 26 (2010) 2337–2342.
[115] Y. Zhao, Y. Cai, J. Tian, H. Lan, Mate. Chem. Phys. 115 (2009) 831–834.
[116] B. Luo, S. Xu, X. Yan, Q. Xue, J. Power Sources 205 (2012) 239–243.
[117] M. Wen, M. Cheng, S. Zhou, Q. Wu, N. Wang, L. Zhou, J. Phys. Chem. C 116 (2012) 11702–11708.
[118] H.P. Liang, L.J. Wan, C.L. Bai, L. Jiang, J. Phys. Chem. B 109 (2005) 7795–7800.
[119] L.V. Shapoval, V.V. Gorbunova, T.B. Boitsova, Russ. J. Gen. Chem. 82 (2012). 1361–1367.
[120] X. Hong, D. Wang, S. Cai, H. Rong, Y. Li, J. Am. Chem. Soc. 134 (2012) 18166–18168.
[121] Karvianto, G.M. Chow, J. Nanopart. Res. 14 (2012) 1186–1205.
[122] J. Ge, W. Xing, X. Xue, C. Liu, T. Lu, J. Liao, J. Phys. Chem. C 111 (2007) 17305–17310.
[123] Z. Liu, B. Zhao, C. Guo, Y. Sun, Y. Sun, Y. Shi, H. Yang, Z. .Li, J. Colloid Interf. Sci. 351 (2010) 233–238.
[124] L. Yi, Y. Song, X. Wang, L. Yi, J. Hu, G. Su, W. Yi, H. Yan, J. Power Sources 205 (2012) 63–70.
[125] Z. Liu, B. Zhao, C. Guo, Y. Sun, F. Xu, H. Yang, Z. Li, J. Phys. Chem. C 223 (2009) 16766–16771.
[126] L. Li, Y. E, J. Yuan, X. Luo, Y. Yang, L. Fan, Electrochim. Acta 56 (2011) 6237–6244.
[127] Z. Bai, L. Yang, J. Zhang, L. Li, J. Lv, C. Hu, J. Zhou, Catal. Commun. 11 (2010) 919–922.
[128] C. Hu, Y. Guo, J. Wang, L. Yang, Z. Yang, Z. Bai, J. Zhang, K. Wang, K. Jiang, ACS Appl. Mater. Interfaces 4 (2012) 4461–4464.
[129] H. Li, J. Liu, S. Xie, M. Qiao, W. Dai, Y. Lu, H. Li, Adv. Funct. Mater. 18 (2008) 3235–3324.
[130] W. Wang, B. Zhao, P. Li, X. Tan, J. Nanopart. Res. 10 (2008) 543–548.
[131] C.L. Lee, C.M. Tseng, R.B. Wu, K.L. Yang, Nanotechnology 19 (2008) 215709–215712.
[132] Y. Jiang, Y. Lu, D. Han, Q. Zhang, L. Niu, Nanotechnology 23 (2012) 105609–105617.
[133] H. Li, Z. Zhu, H. Li, P. Li, X. Zhou, J. Colloid Interf. Sci. 349 (2010) 613–619.
[134] Y.G. Sun, Y.N. Xia, Science 298 (2002) 2176–2179.
[135] Z. Sun, J. Masa, W. Xia, D. König, A. Ludwig, Z.A. Li, M. Farle, W. Schuhmann, M. Muhler, ACS Catal. 2 (2012) 1647–1653.
[136] C. Zhu, S. Guo, S. Dong, Adv. Mater. 24 (2012) 2326–2331.